

N O T I C E

THIS DOCUMENT HAS BEEN REPRODUCED FROM
MICROFICHE. ALTHOUGH IT IS RECOGNIZED THAT
CERTAIN PORTIONS ARE ILLEGIBLE, IT IS BEING RELEASED
IN THE INTEREST OF MAKING AVAILABLE AS MUCH
INFORMATION AS POSSIBLE

(NASA-CR-168395) HOLOGRAPHIC INTERFEROMETRY
OF TRANSPARENT MEDIA WITH REFLECTION FROM
IMBEDDED TEST OBJECTS (Michigan Univ.) 26 p
HC A03/MF A01 CSCL 14E

N82-17475

Unclas

G3/35 08841



College of Engineering

**Department of
Mechanical Engineering
& Applied Mechanics**

The University of Michigan

Ann Arbor, Michigan 48109



I N T F L 8103

HOLOGRAPHIC INTERFEROMETRY OF TRANSPARENT
MEDIA WITH REFLECTION FROM IMBEDDED
TEST OBJECTS

I. Prikryl

C. M. Vest

October 1981

Interferometry Laboratory
Department of Mechanical Engineering
and Applied Mechanics
The University of Michigan
Ann Arbor, Michigan 48109

Prepared for the National Aeronautics and Space Administration

Ames Research Center

Grant No. NAG 2-118

1. INTRODUCTION

It is possible to measure 2-or 3-dimensional refractive index distributions in transparent media by recording data using holographic interferometry and analyzing this data by the techniques of computer tomography. Interference fringe patterns corresponding to each of several different viewing directions provide a set of measured values of line integrals through the transparent medium. Given a set of such values of line integrals, the procedures of computer tomography enable one to compute an estimate, referred to as a reconstruction, of the 2-or 3-dimensional refractive index distribution. This combined technique has application to experimentation in fields such as aerodynamics, heat transfer, plasma diagnostics, and stress analysis of transparent solids.

A variety of techniques and computer algorithms for effecting such reconstructions are indicated in ref. 1 for the practical case in which the data are discreet and the number of viewing directions is finite. Several researchers have dealt with the problem of accurate estimation of reconstructions when the range of viewing directions is less than 180° . (See for example, ref. 2.)

A difficult problem of considerable practical importance occurs when an opaque object is present within the field under study. For example, in aerodynamic testing the test model about which flow is being studied blocks a portion of the optical beam used to form the interferogram. This gives rise to incomplete data for standard computer tomography algorithms. It is with this case that this paper is concerned.

Reconstruction techniques for the case of tomography when an opaque object blocks part of the field of view have been proposed by Bates, et al ³, Zien, et al ⁴, and Vest, et al ⁵. The common feature of these computational approaches is to define either directly ^{3,4} or indirectly ⁵, a continuation of the unknown density field into the space occupied by the opaque object. This continuation, which is effected according to some physical or mathematical criteria, then makes it possible to compute projections through the space occupied by the opaque object. The problem is thereby transformed to one of ordinary tomography prior to reconstruction.

In the present paper, which is presented entirely in the context of holographic interferometry, we propose an experimental technique for circumventing the problem of data blocked by opaque objects. The technique is simple in principle; the "missing" data are completed by forming an interferogram using light backscattered from the opaque object, which is assumed to be diffuse. The remainder of the data can be recorded by the normal techniques of transmission holographic interferometry. Because the test object, whose shape is considered to be arbitrary, is by necessity assumed to be diffuse, an interesting problem of fringe localization arises. This is discussed in the following sections.

2. TECHNIQUE AND FRINGE FORMATION

In order to fill in the "missing" data for a particular viewing direction, we consider the object to be illuminated by a plane wave of laser light propagating in the negative z direction. The origin of the z axis is considered to be attached to the object and pointing toward the observer. One

exposure of a double-exposure hologram is recorded when the medium surrounding the object has a uniform refractive index n_0 . The other exposure is recorded while the refractive index distribution $n(x,y,z)$ is present. The resulting holographic interferogram is viewed using an optical system which spatially filters the light so that one observes only rays traveling in the z direction. Two characteristics of the interferogram formed in this manner must be kept in mind. First, the light is diffuse and therefore fringe localization will occur when the viewing aperture is finite. Second, we are dealing with a double-pass interferometer, i.e. the observed light has passed through the unknown refractive index field twice, first in the the negative z direction and then in the positive z direction.

Equations for the localization of fringes of holographic interferometry in a diffusely back-illuminated refractive index field are derived and presented in ref. 6. A simple geometrical optics approach is used, ray bending due to refraction is assumed to be negligible, and the position of fringe localization is defined by the distance z_L from an arbitrary coordinate origin along the viewing direction to the point in space where the fringes of holographic interferometry have maximum visibility. The region of fringe localization depends only on the structure of the unknown refractive index field; it is independent of the location of the entrance pupil of the observing system relative to the diffuser. This is in strong contrast to the case of fringe localization in a holographic interferogram of a displaced or deformed diffusely-reflecting opaque object (see for example ref. 7).

We have derived the equations describing fringe localization for the double-pass holographic interferometer described above. Because the derivation is so similar to that presented in Ref. 6, it is not repeated here. The resulting equations of fringe localization are:

$$z_L = \frac{\int \frac{\partial f(x, y, z)}{\partial x} z dz}{2 \int \frac{\partial f(x, y, z)}{\partial x} dz} \quad (1a)$$

$$z_L = \frac{\int \frac{\partial f(x, y, z)}{\partial y} z dz}{2 \int \frac{\partial f(x, y, z)}{\partial y} dz} \quad (1b)$$

In these equations $f(x, y, z) = n(x, y, z) - n_0$ is the change of the refractive index field between holographic exposures. Eqs. 1a and 1b differ in form from those given in Ref. 6 for the single-pass case only by the presence of the factor 2 in the denominators. The reader should note, however, that in the present case, the origin of the z axis is attached to the diffuse object. Furthermore, because the shape of the object is arbitrary, these equations must be applied to each principal ray separately.

Interferograms formed in the manner under consideration differ from those formed by the standard back-illumination procedure in two ways. First, the double-pass interferogram has twice the sensitivity, i.e. the number of fringes will be doubled relative to that for a single-pass interferogram. Second, Eqs. 1a and 1b indicate that fringes localize in a surface

half way between the diffuser and the region of localization for the single-pass case. This change in localization is actually desirable, because it indicates that the surface of fringe localization will be compressed by a factor of 2. This can be important because localization surfaces occurring in interferometry of transparent media can be very convoluted. The compression makes it possible to photograph the fringes with a larger aperture, thereby reducing speckle noise.

3. EXPERIMENTAL VERIFICATION

In order to verify the correctness of the above analysis, the experimental apparatus shown schematically in Fig. 1, and photographically in Figs. 2 and 3, was constructed. The refractive index field under study was generated by two natural convective plumes rising in the air above electrical heating elements each having a diameter of 8mm. The heating elements which dissipated identical amounts of energy, were separated by 50mm and located at a distance Z from the plane diffuser D . The beam splitter B and lens L were arranged so that the object could be illuminated by a plane wave propagating toward the diffuser, i.e. in the negative z direction. After being scattered by the diffuser, this light traversed the refractive index distribution in the opposite direction, passed back through the beam splitter B and impinged on the holographic plate H . For simplicity, the reference wave has been omitted from Fig. 1. Double exposure holograms were recorded using this apparatus. The resulting holographic interferograms were viewed with the aid of an imaging system which had a circular aperture stop A located in the focal plane

of lens L. This aperture stop restricted the rays used to form the interferogram to those which traveled parallel to the original illumination beam.

Two reflective diffusers were used during this investigation. One was a plane diffuser located at a distance $Z=90\text{mm}$ from the heating elements, and the other was an object of more complex shape located at a distance $Z=630\text{mm}$ from the heating elements. For each of these diffusers a sequence of interferograms were recorded with the imaging system focused on planes $z=0$, $z=Z/2$ and $z=Z$. Because the individual thermal plumes were radially symmetric, the fringes were predicted to be localized in a surface at a approximately $z=Z/2$. The numerical aperture of the imaging system was also varied during the experiment. Figs. 4 through 7 were made with the plane diffuser located at a distance $Z=90\text{mm}$ from the heating elements and for the numerical apertures of 0.04, 0.02, 0.01, and 0.005, respectively. Figs. 8 through 11 were recorded for the same sequence of numerical apertures with the plane diffuser located at a distance $Z=630\text{mm}$ from the heating elements. Figs. 12 through 15 were recorded for the same sequence of apertures using a diffuser of more general shape located approximately 630mm from the heating elements. Examination of these interferograms indicates that when they are formed using a small to moderate aperture, the fringes are indeed found to be localized in the vicinity of the plane $z=Z/2$ as predicted theoretically.

During this investigation an interesting phenomenon was observed. As expected, when the distance Z was large, i.e. $Z=630\text{mm}$, fringes photographed in the plane of localization, $z=Z/2$, were found to be rather blurred if the

numerical aperture was large (N.A.=0.04). Although the fringes in this case had poor visibility, their number and position were the same as when formed with a more optimal aperture. However, when the interferogram was photographed using an imaging system focused at a large distance from the surface of localization, for example $z=0$ or $z=630\text{mm}$, the numbers of fringes in the interferogram appeared to be approximately one-half the number in the surface of localization. Clearly, if data were recorded in this manner it would be unacceptable for quantitative evaluation.

The explanation of this phenomenon is as follows. High quality fringes are formed only if all of the ray pairs admitted by the aperture and contributing to the interference pattern at a particular point in the interferogram have undergone nearly the same phase shift. When the aperture is sufficiently large, this criterion will not be met and the phase difference over these ray pairs may exceed π substantially if the imaged plane is far from the surface of localization. In this case the fringe pattern can be thought of as the superposition of fields admitted by an ensemble of small apertures filling the entrance pupil. If the plane being imaged is sufficiently far from the surface of localization an apparent change in the number of fringes can occur.

4. CONCLUSIONS

We have proposed that interferometric data which are ordinarily blocked by an opaque object within the field under study can be recorded using light scattered by the surface of this opaque object. When interferograms are recorded in this manner, the fringe localization surface is compressed and displaced, and the number of interference fringes is doubled. The compression of the localization surface enables the observer to use a larger numerical

aperture then would be possible otherwise. However, it is necessary to focus the imaging system close to the surface of fringe localization and to use a numerical aperture which is not so large as to cause degradation of the fringe pattern.

References

1. R. Gordon and G. T. Herman, Three-dimensional reconstruction from projections: a review of algorithms, *Int. Rev. Cytology*, 38, 111-151 (1974).
2. T. Sato, S. J. Norton, M. Linser, O. Ikeda, and M. Hirama, Tomographic image reconstruction from limited projections using iterative revisions in image and transform spaces, *Appl. Opt.*, 20, 395-399 (1981).
3. R. H. T. Bates, R. M. Lewitt, T. M. Peters, and P. R. Smith, Image reconstruction from incomplete projections, in *Image Processing for 2-D and 3-D Reconstruction from Projections: Theory and Practice in Medicine and the Physical Sciences*, Tech. Digest of Topical Meeting, Stanford, CA, 1975, publ. by Opt. Soc. Am. (1976).
4. T. F. Zien, W. C. Ragsdale, and W. C. Spring, III, Quantitative determination of three-dimensional density field by holographic interferometry, *AIAA J.*, 13, 841-842 (1975).
5. C. M. Vest, S. Cha, and P. Farrell, Measurement of three-dimensional temperature fields by holographic interferometry, Rept. No. INTFL 80, Interferometry Laboratory, Dept. of Mechanical Engineering & Applied Mechanics, The Univ. of Michigan, Ann Arbor (1980).
6. C. M. Vest, *Holographic Interferometry*, Wiley, New York (1979).
7. I. Prikryl, Localization of interference fringes in holographic interferometry, *Optica Octa*, 21, 675-681 (1974).

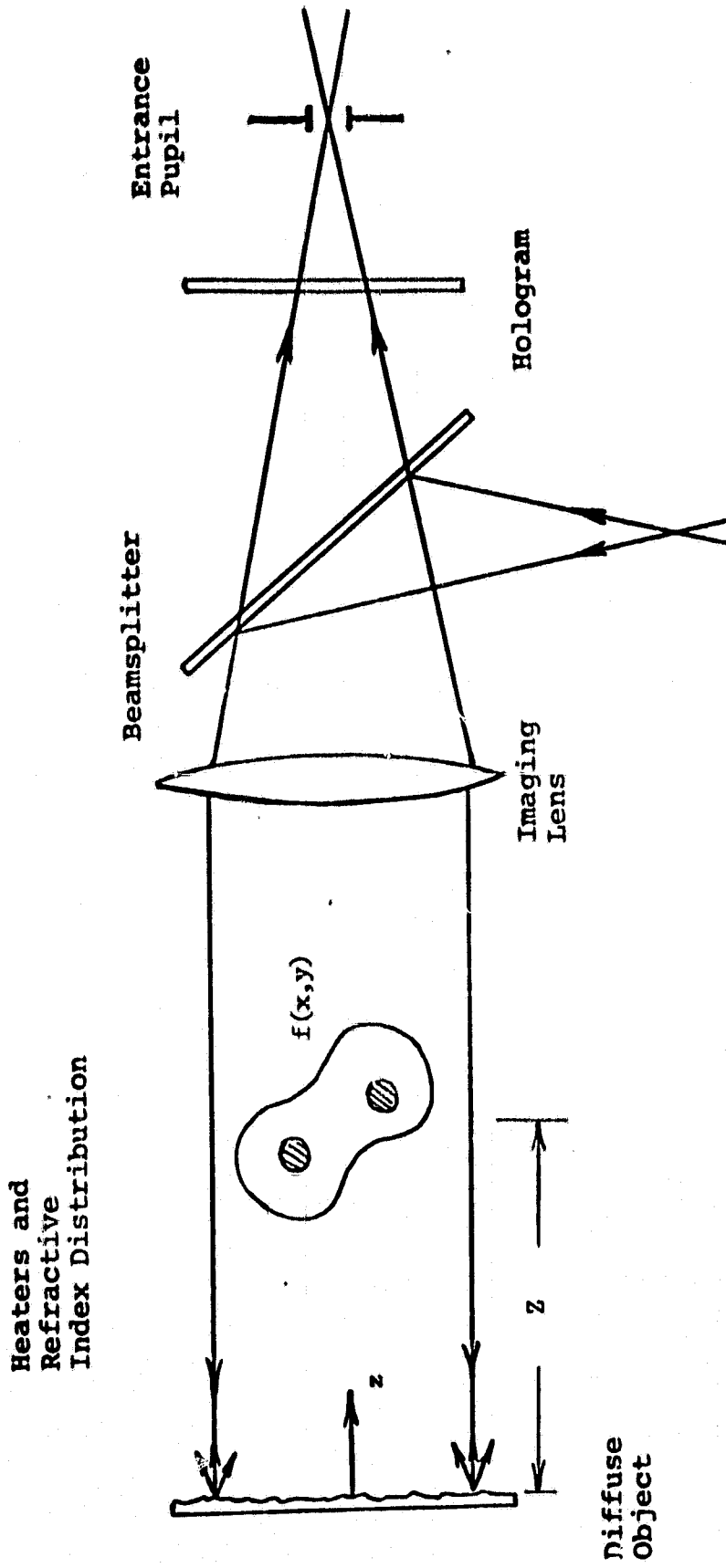


Fig. 1. Optical apparatus for recording holographic interferograms of a refractive index distribution with forward illuminations of a diffuse object in the field.

ORIGINAL PAGE
BLACK AND WHITE PHOTOGRAPH

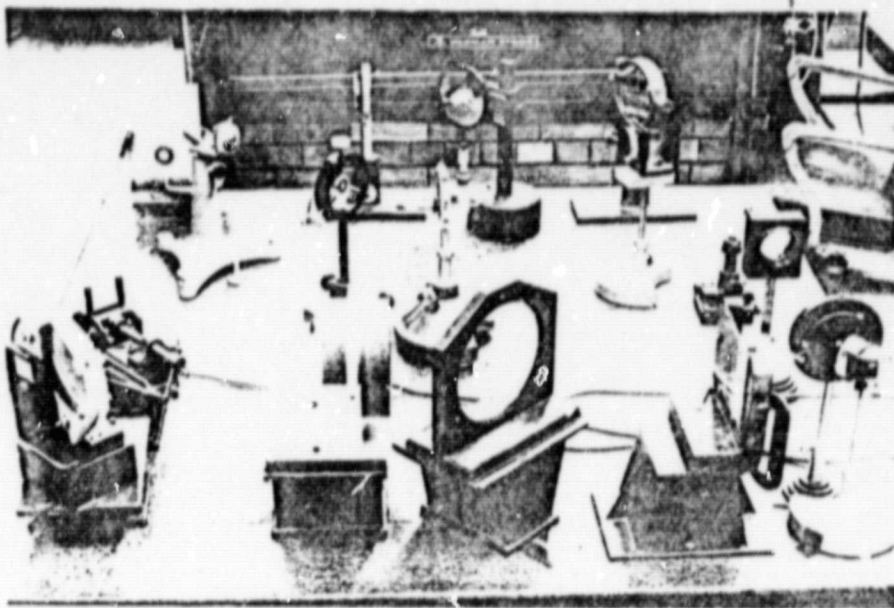


Fig. 2. Experimental setup.

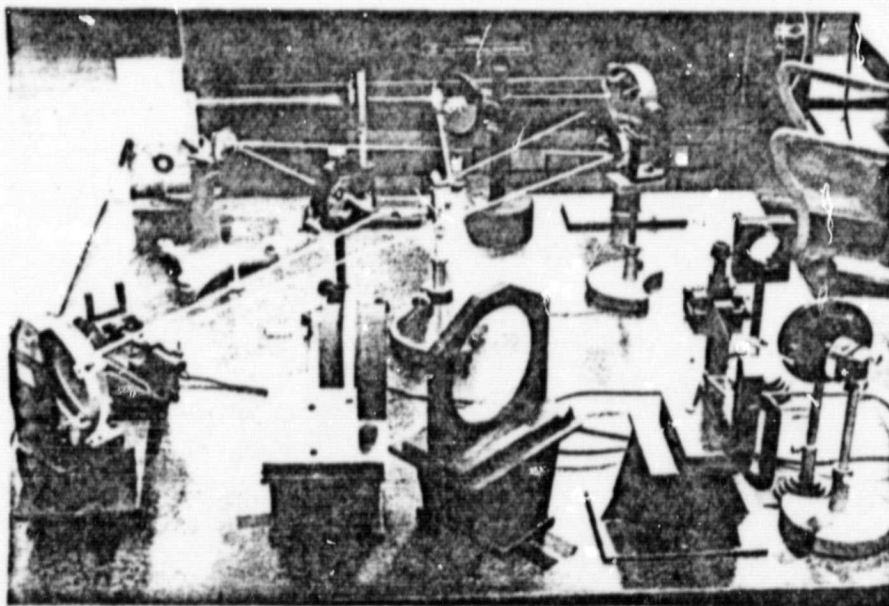
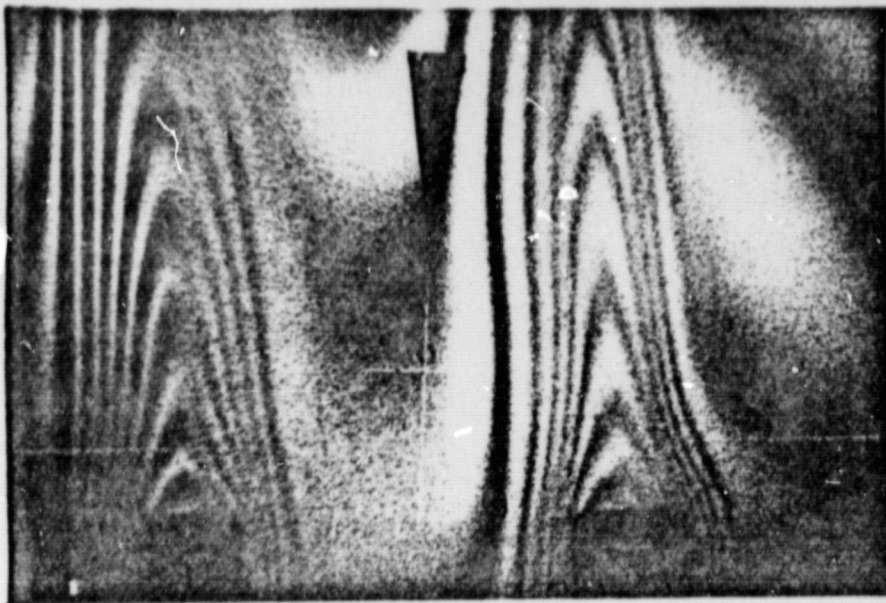
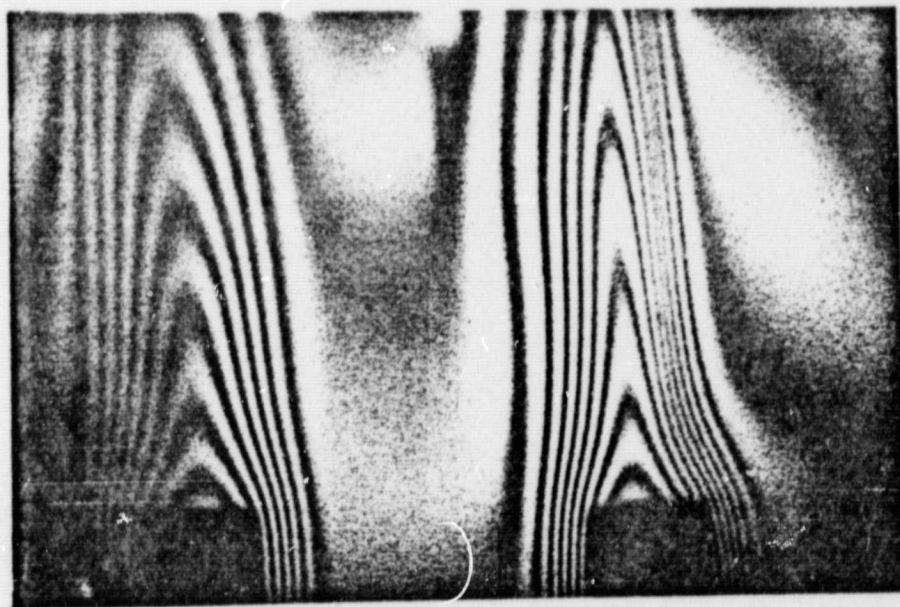


Fig. 3. Another view of experimental setup.

ORIGINAL PAGE
BLACK AND WHITE PHOTOGRAPH



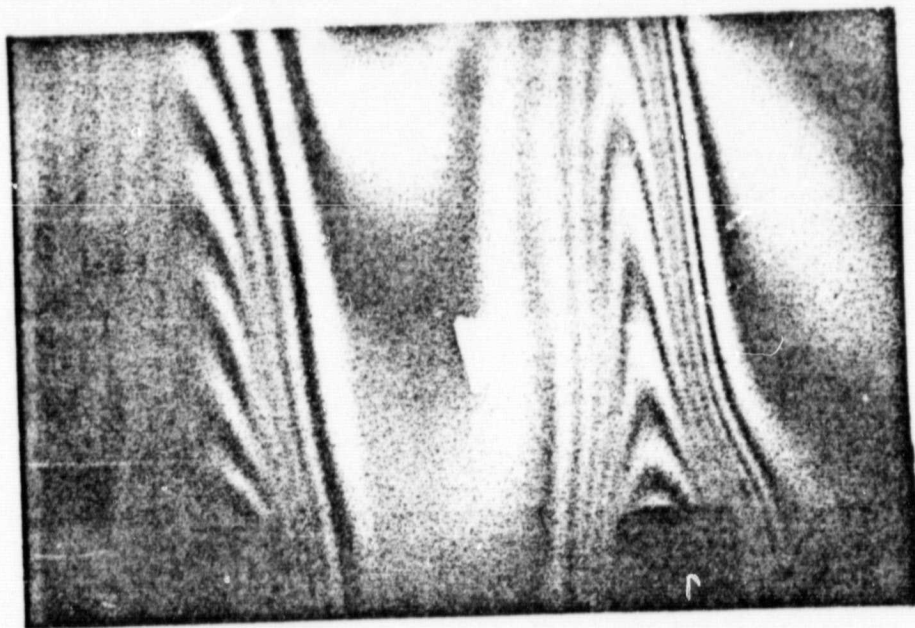
(a) $z=0$



(b) $z=z/2$

Fig. 4. Interferograms recorded with plane diffuser at $z=90\text{mm}$, and numerical aperture=0.04.

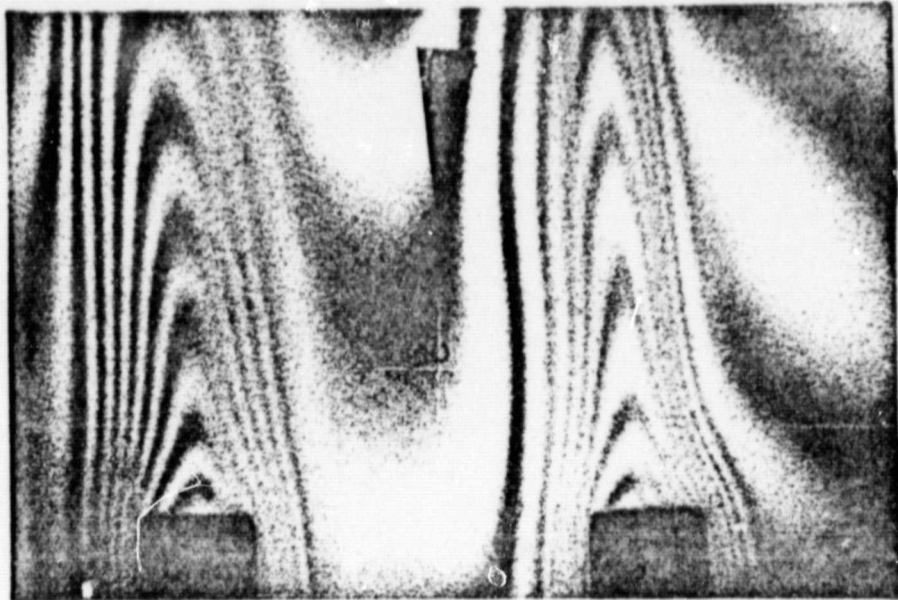
ORIGINAL PAGE
BLACK AND WHITE PHOTOGRAPH



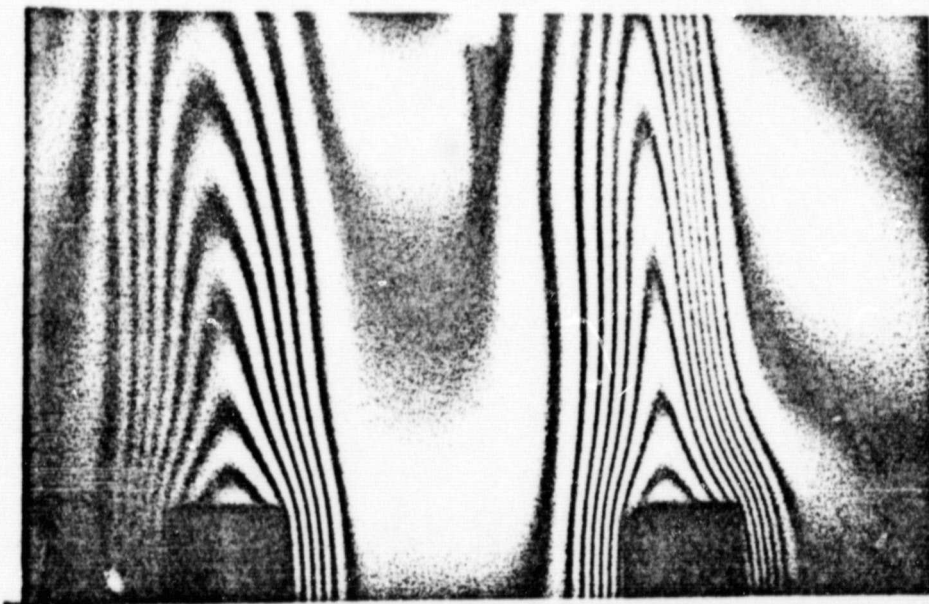
(c) $z=Z$

Fig. 4 (cont'd)

ORIGINAL PAGE
BLACK AND WHITE PHOTOGRAPH



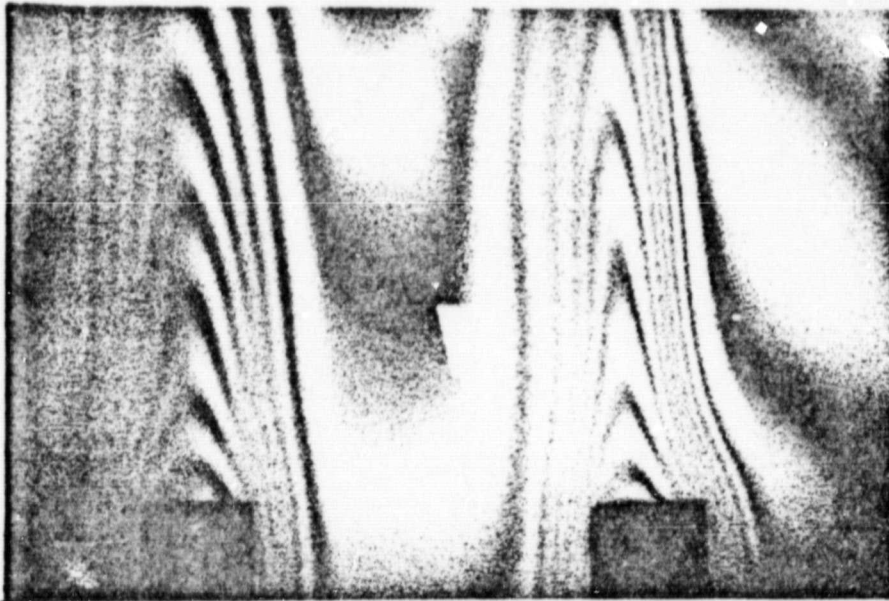
(a) $z=0$



(b) $z=z/2$

Fig. 5. Interferograms recorded with plane diffuser at $z=90\text{mm}$, and numerical aperture=0.02.

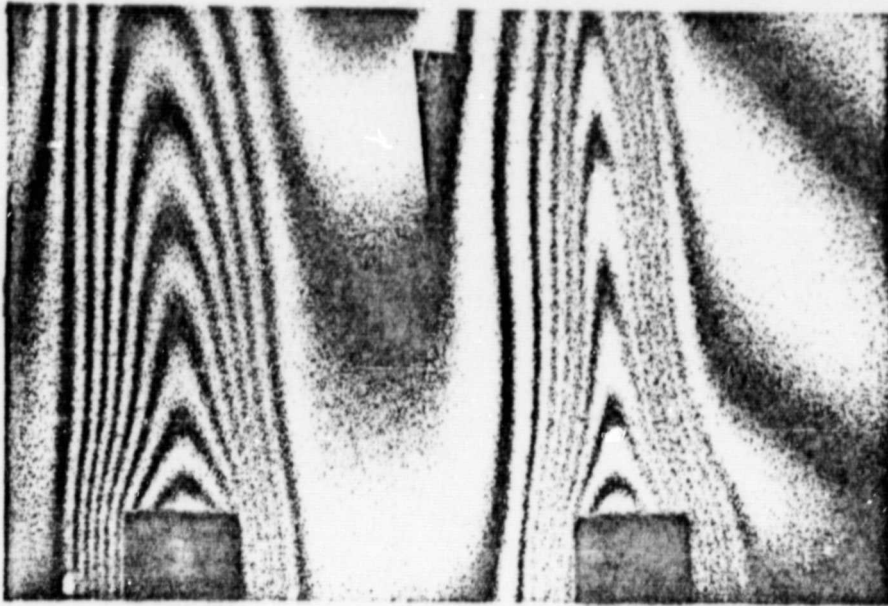
ORIGINAL PAGE
BLACK AND WHITE PHOTOGRAPH



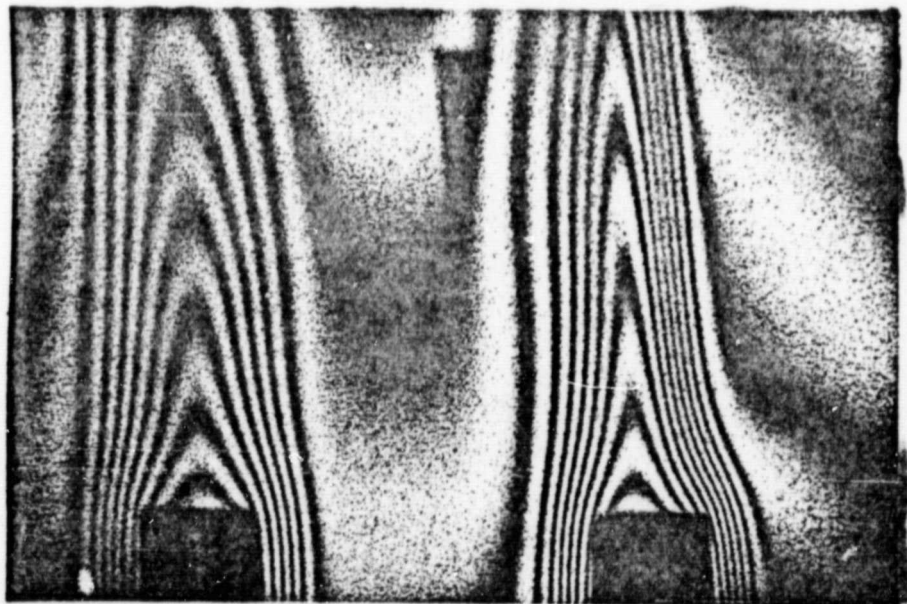
(c) $z=Z$

Fig. 5 (cont'd)

ORIGINAL PAGE
BLACK AND WHITE PHOTOGRAPH



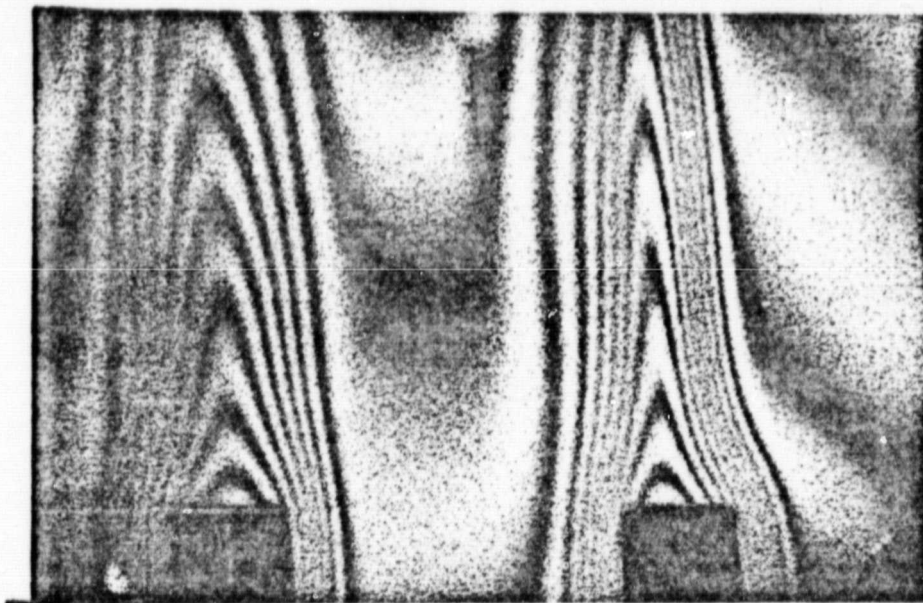
(a) $z=0$



(b) $z=z/2$

Fig. 6. Interferograms recorded with plane diffuser at $Z=90\text{mm}$, and numerical aperture=0.01.

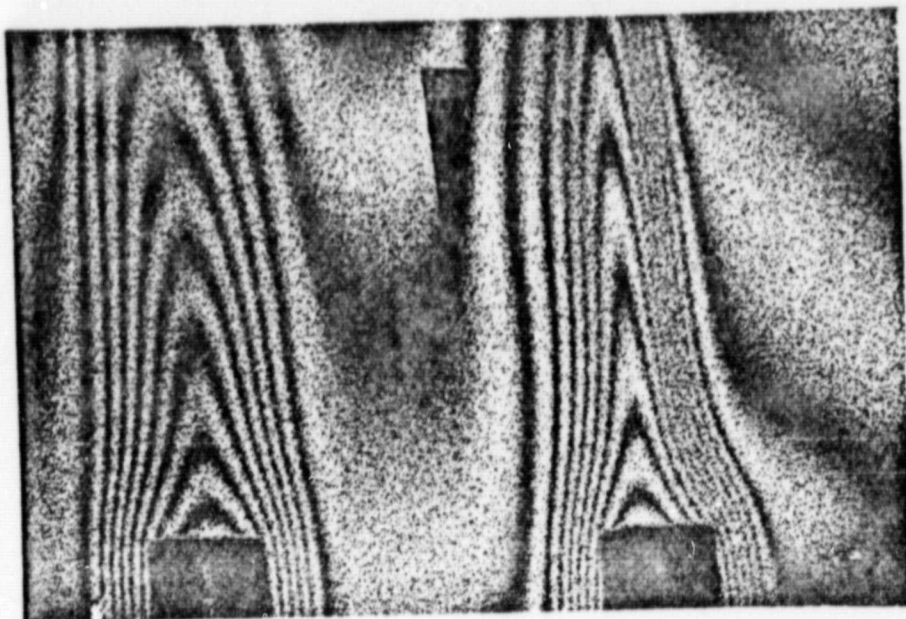
ORIGINAL PAGE
BLACK AND WHITE PHOTOGRAPH



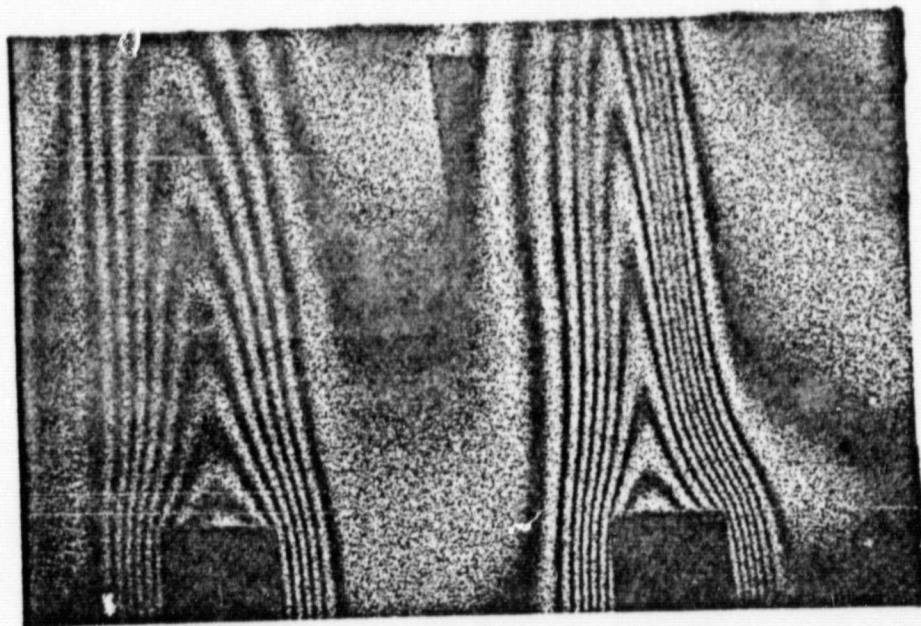
(c) $z=Z$

Fig. 6 (continued)

ORIGINAL PAGE
BLACK AND WHITE PHOTOGRAPH



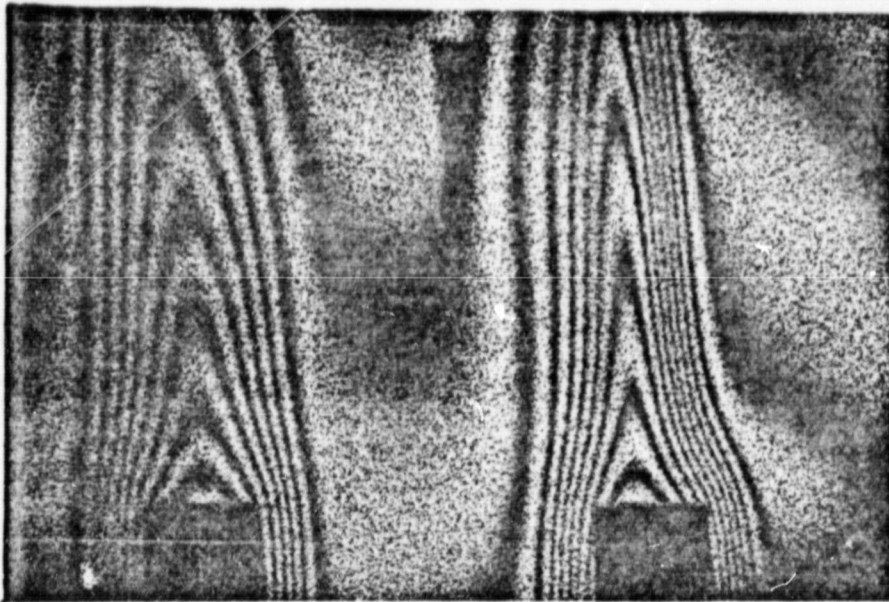
(a) $z=0$



(b) $z=z/2$

Fig. 7. Interferograms recorded with plane diffuser at $z=90\text{mm}$, and numerical aperture=0.005.

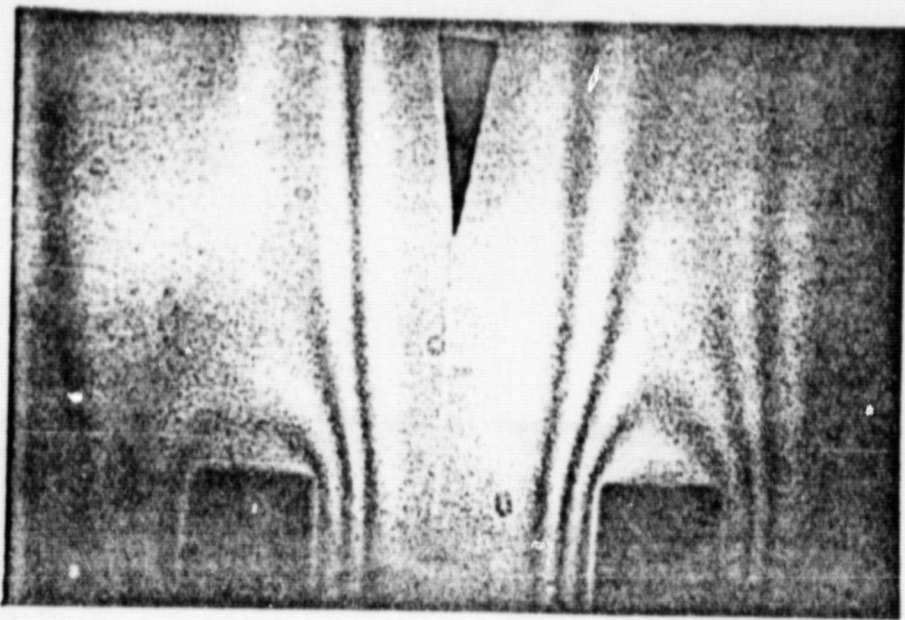
ORIGINAL PAGE
BLACK AND WHITE PHOTOGRAPH



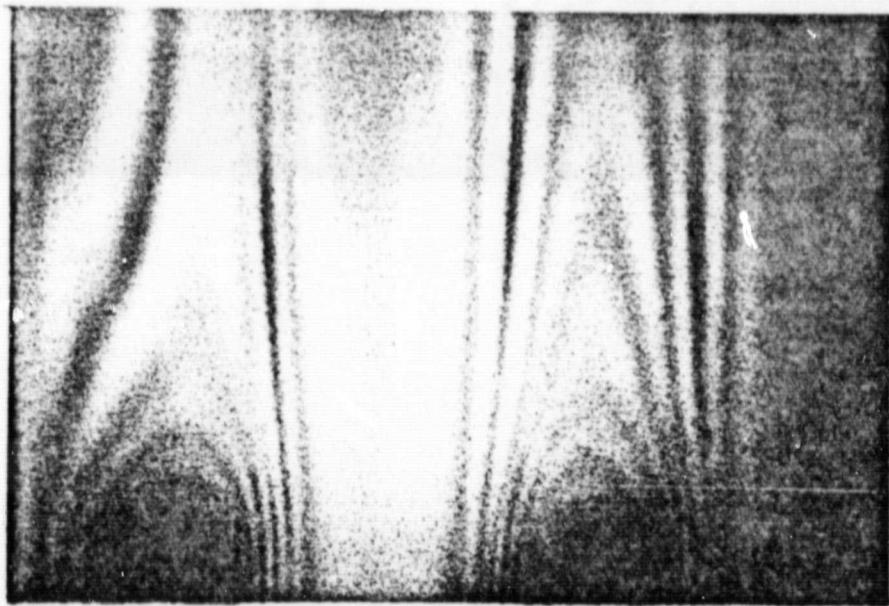
(c) $z=Z$

Fig. 7 (continued)

ORIGINAL PAGE
BLACK AND WHITE PHOTOGRAPH



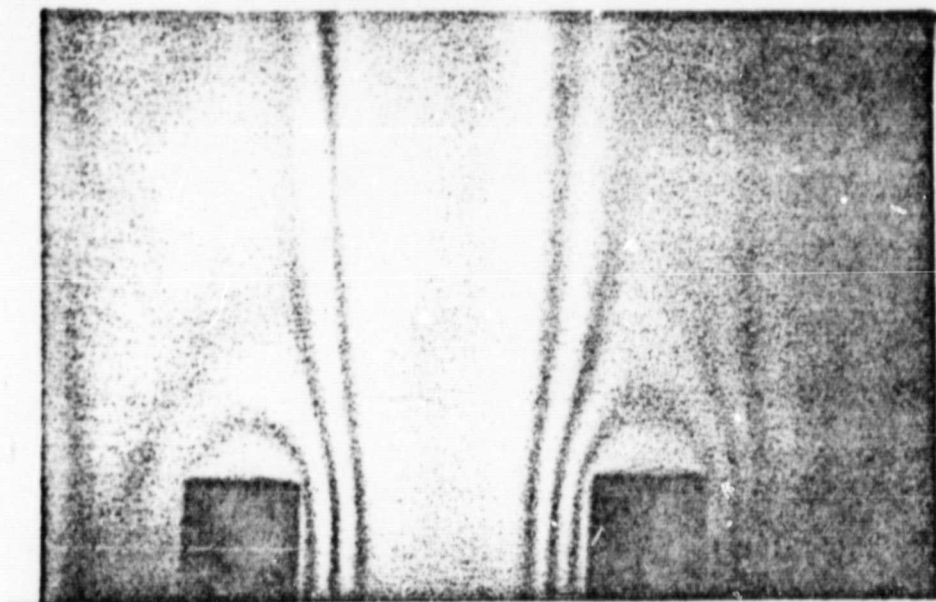
(a) $z=0$



(b) $z=z/2$

Fig. 8. Interferograms recorded with plane diffuser at $Z=630\text{mm}$, and numerical aperture=0.04

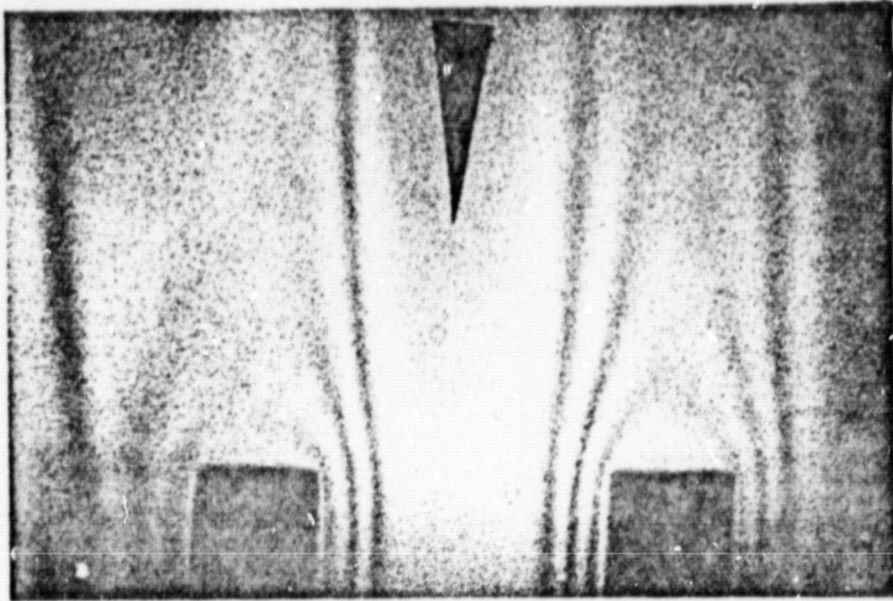
ORIGINAL PAGE
BLACK AND WHITE PHOTOGRAPH



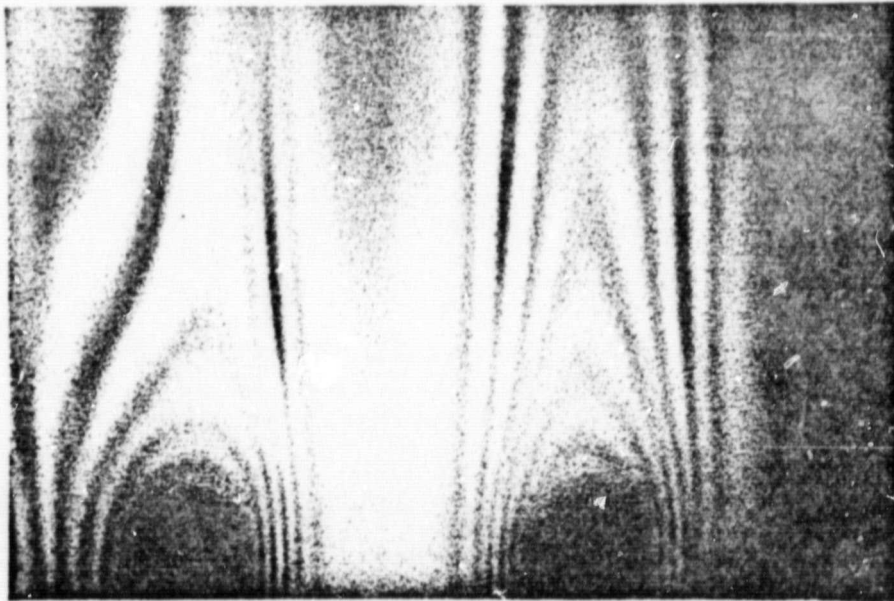
(c) $z=Z$

Fig. 8 (continued)

ORIGINAL PAGE
BLACK AND WHITE PHOTOGRAPH



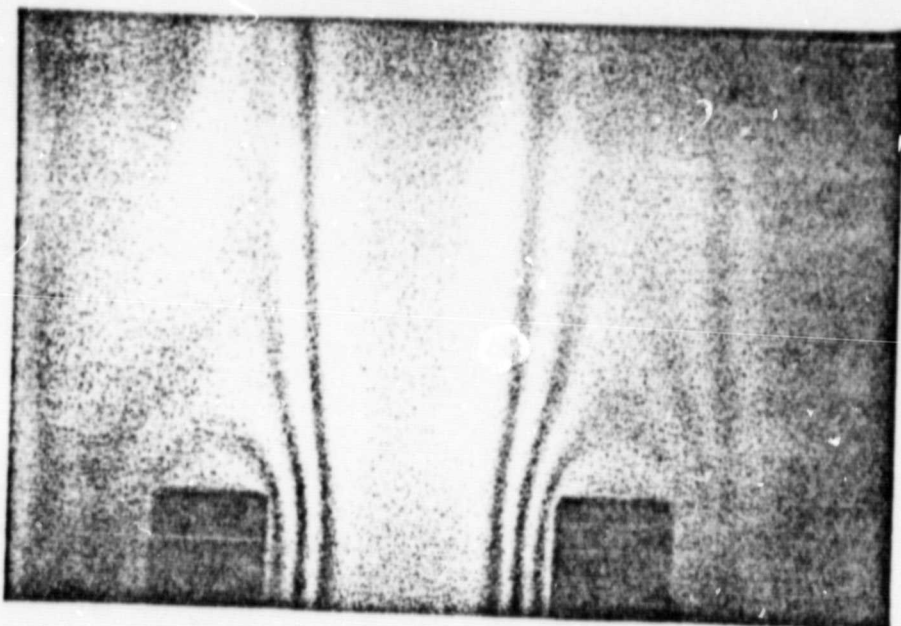
(a) $z=0$



(b) $z = Z/2$

Fig. 9. Interferograms recorded with plane diffuser at $Z=630\text{mm}$, and numerical aperture=0.02.

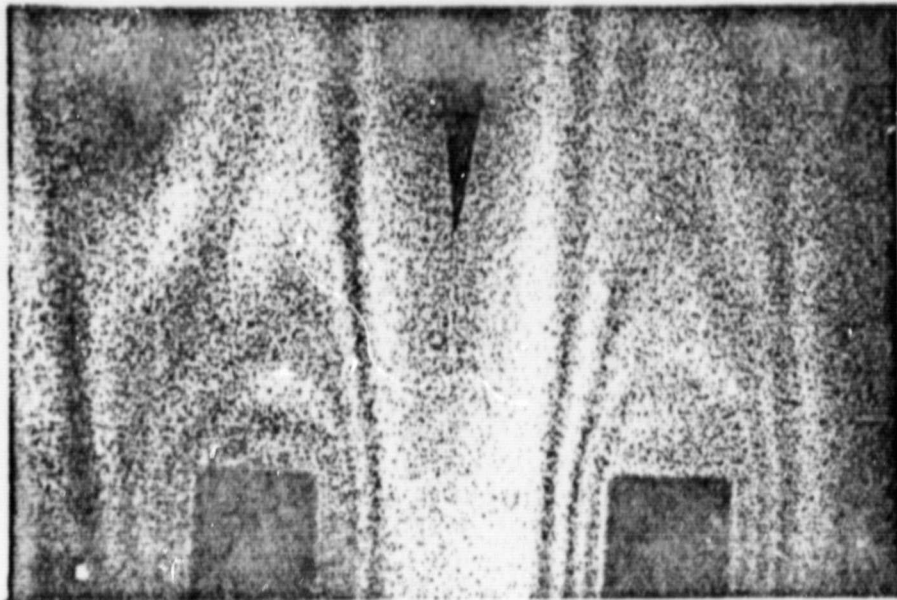
ORIGINAL PAGE
BLACK AND WHITE PHOTOGRAPH



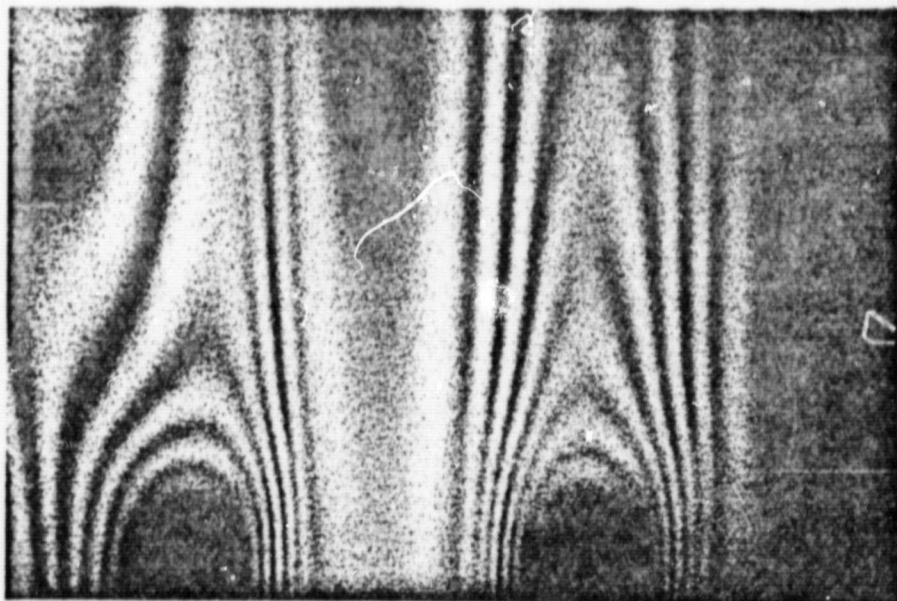
(c) $z=Z$

Fig. 9. (continued)

ORIGINAL PAGE
BLACK AND WHITE PHOTOGRAPH



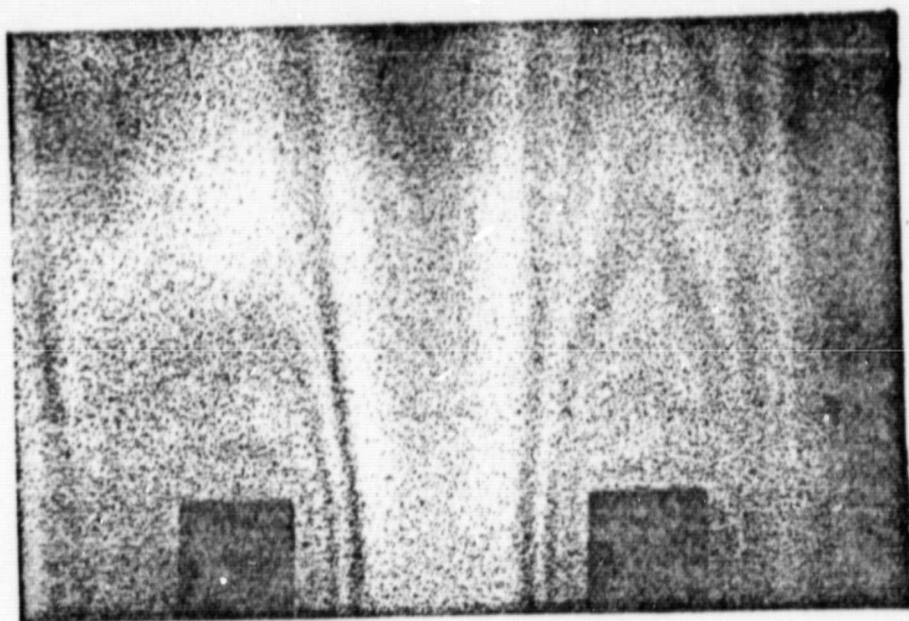
(a) $z=0$



(b) $z=z/2$

Fig. 10. Interferograms recorded with plane diffuser at $Z=630\text{mm}$, and numerical aperture=0.01.

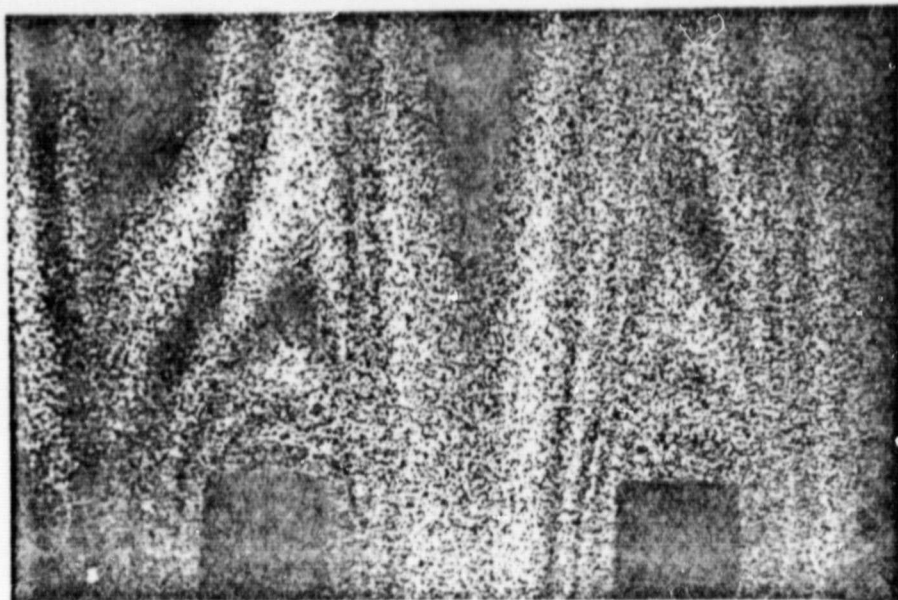
ORIGINAL PAGE
BLACK AND WHITE PHOTOGRAPH



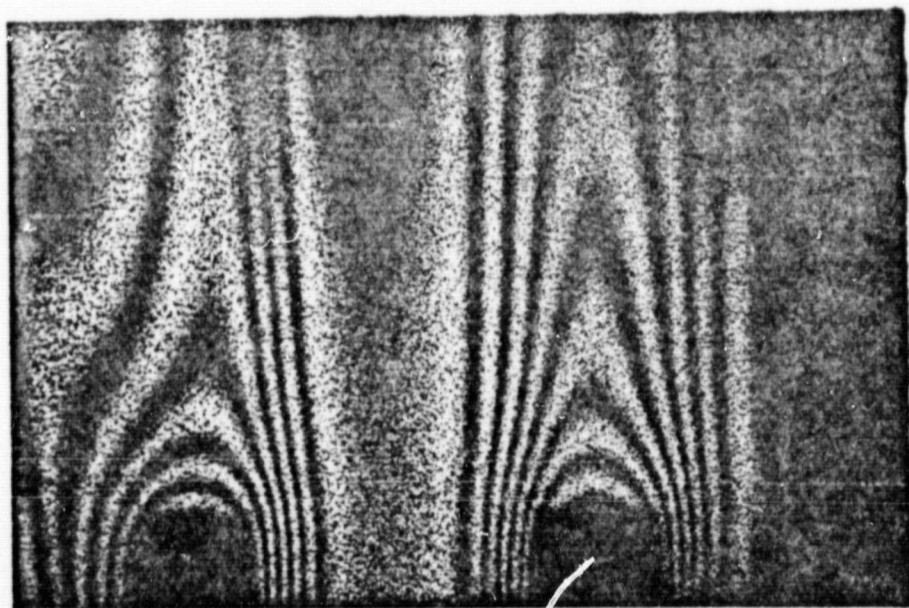
(c) $z=Z$

Fig. 10 (continued)

ORIGINAL PAGE
BLACK AND WHITE PHOTOGRAPH



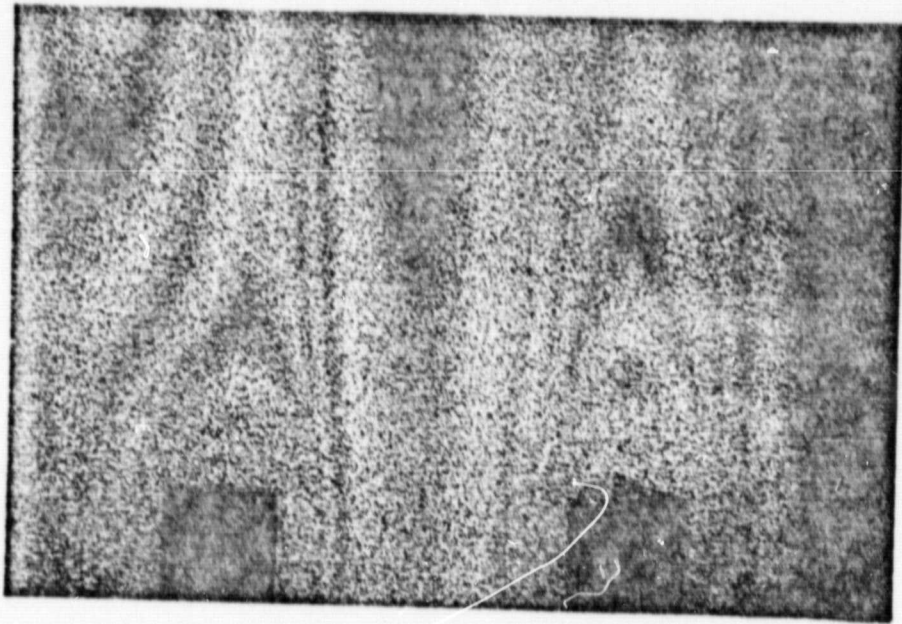
(a) $z=0$



(b) $z=z/2$

Fig. 11. Interferograms recorded with plane diffuser at $Z=630\text{mm}$, and numerical aperture=0.005.

ORIGINAL PAGE
BLACK AND WHITE PHOTOGRAPH



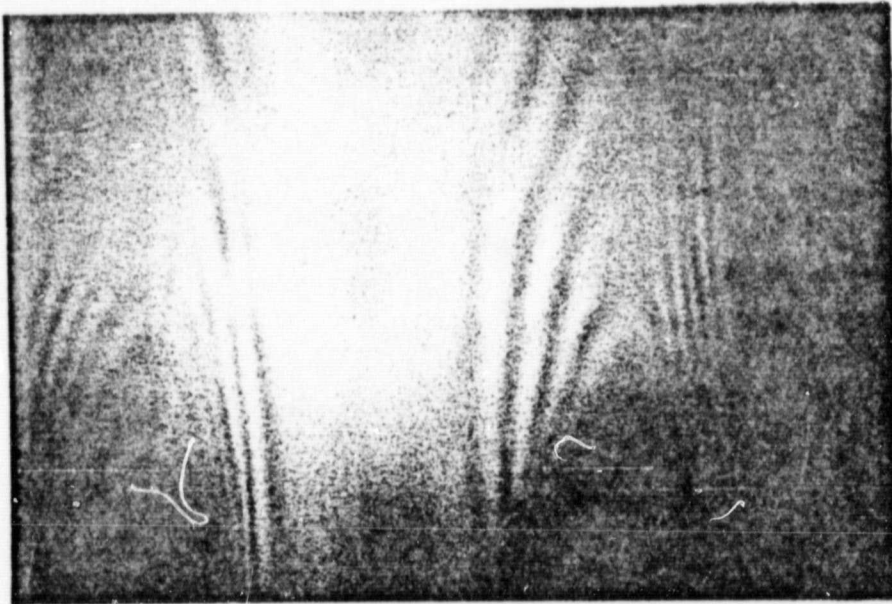
(c) $z=Z$

Fig. 11 (continued)

ORIGINAL PAGE
BLACK AND WHITE PHOTOGRAPH



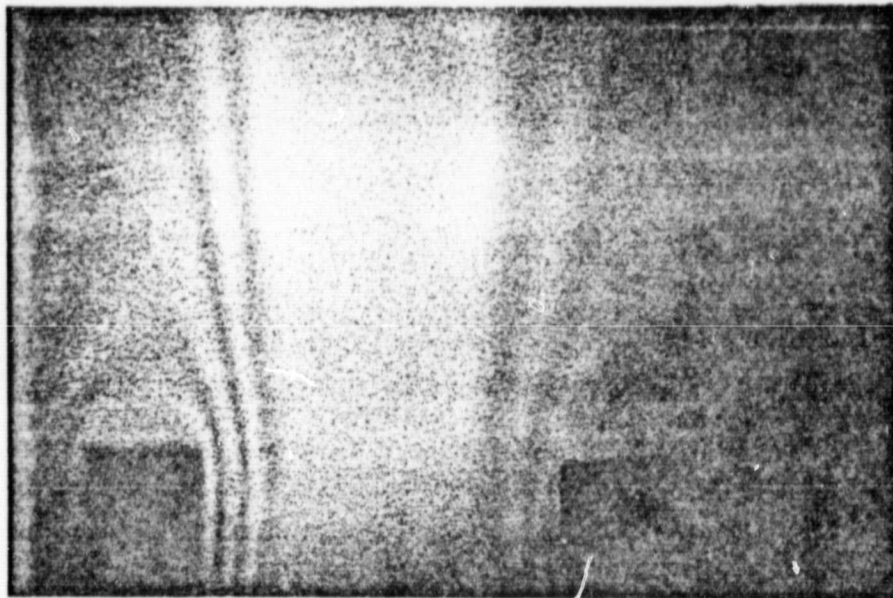
(a) $z=0$



(b) $z=z/2$

Fig. 12, Interferograms recorded with three-dimensional diffuser at $Z=630\text{mm}$, and numerical aperture=0.01.

ORIGINAL PAGE
BLACK AND WHITE PHOTOGRAPH



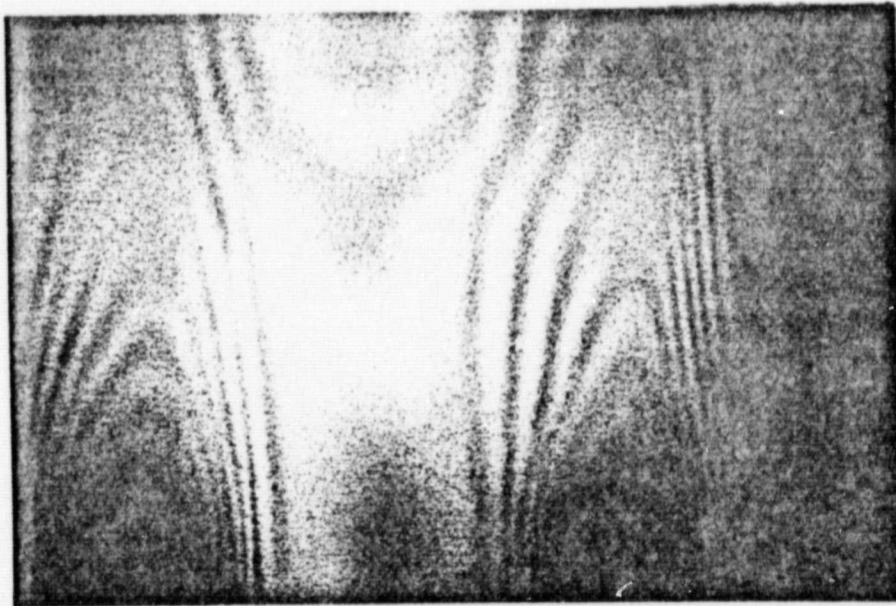
(c) $z=Z$

Fig. 12, (continued)

ORIGINAL PAGE
BLACK AND WHITE PHOTOGRAPH



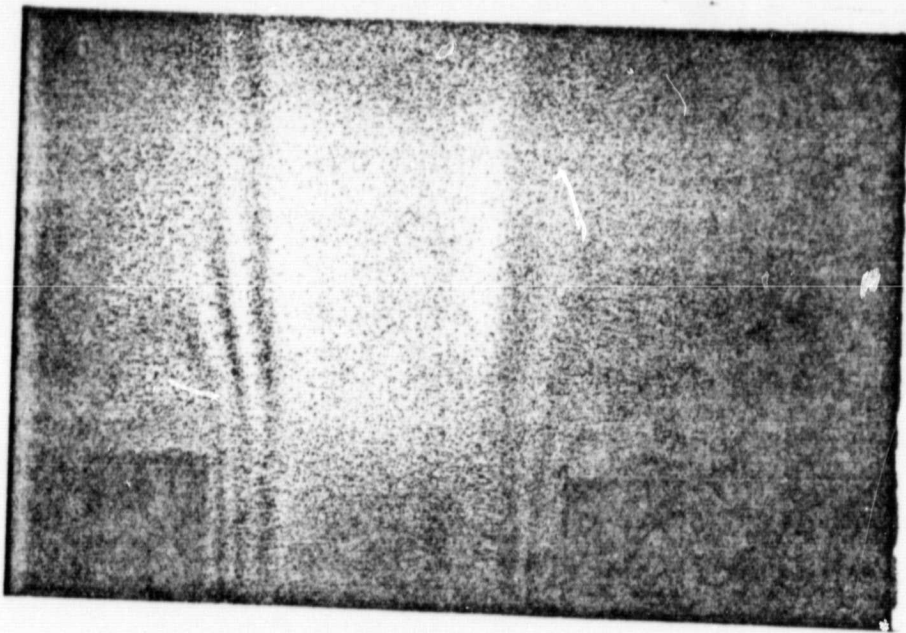
(a) $z=0$



(b) $z=z/2$

Fig. 13. Interferograms recorded with three-dimensional diffuser at $Z=630\text{mm}$, and numerical aperture=0.02.

ORIGINAL PAGE
BLACK AND WHITE PHOTOGRAPH



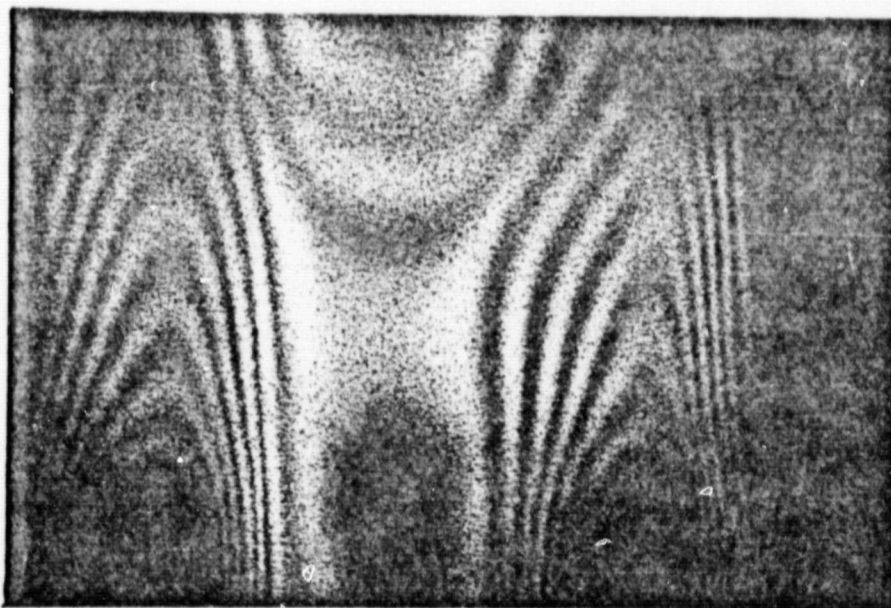
(c) $z=Z$

Fig. 13 (continued)

ORIGINAL PAGE
BLACK AND WHITE PHOTOGRAPH



(a) $z=0$



(b) $z=z/2$

Fig. 14. Interferograms recorded with three-dimensional diffuser at $Z=630\text{mm}$, and numerical aperture=0.01.

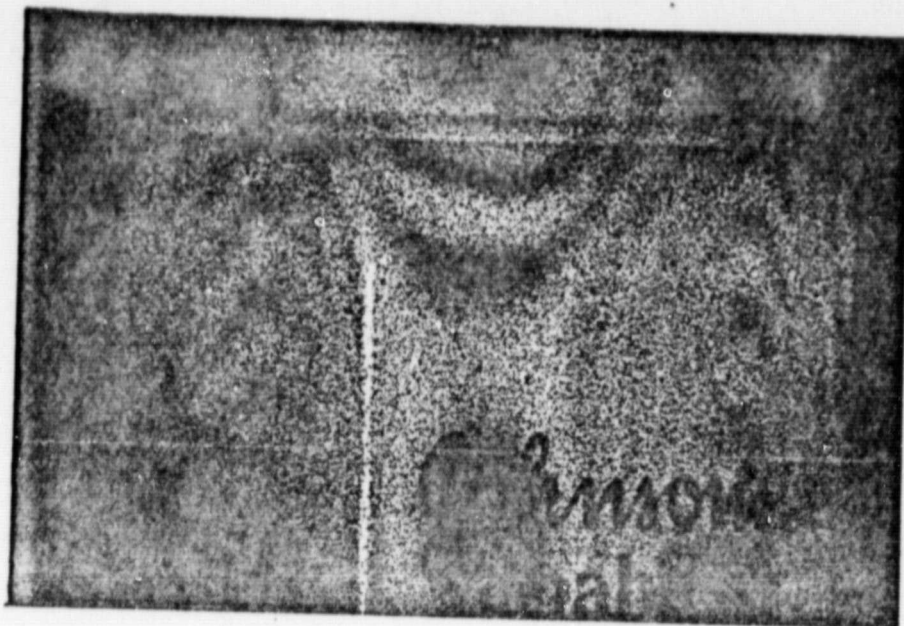
ORIGINAL PAGE
BLACK AND WHITE PHOTOGRAPH



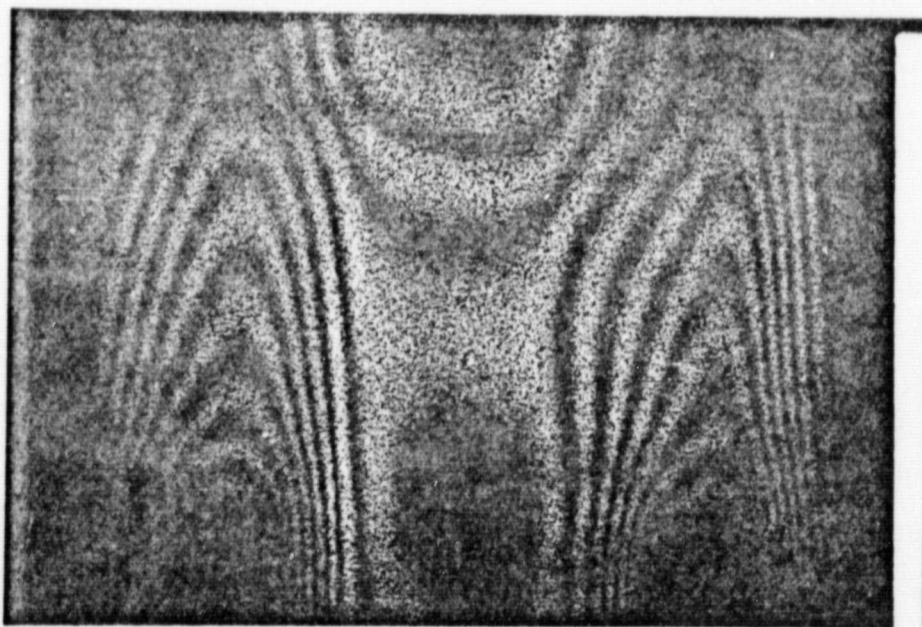
(c) $z=Z$

Fig. 14 (continued)

ORIGINAL PAGE
BLACK AND WHITE PHOTOGRAPH



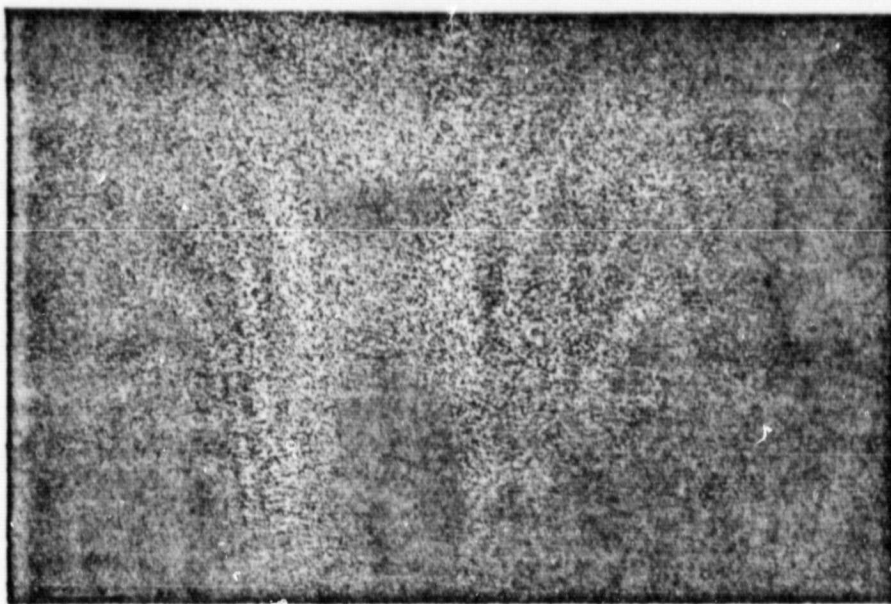
(a) $z=0$



(b) $z=z/2$

Fig. 15. Interferograms recorded with three-dimensional diffuser at $Z=630\text{mm}$, and numerical aperture=0.005.

ORIGINAL PAGE
BLACK AND WHITE PHOTOGRAPH



(c) $z=Z$

Fig. 15 (continued)